

Activation of Si implants into InAs characterized by Raman scattering

A. G. Lind, T. P. Martin Jr., V. C. Sorg, E. L. Kennon, V. Q. Truong, H. L. Aldridge, C. Hatem, M. O. Thompson, and K. S. Jones

Citation: [Journal of Applied Physics](#) **119**, 095705 (2016); doi: 10.1063/1.4942880

View online: <http://dx.doi.org/10.1063/1.4942880>

View Table of Contents: <http://scitation.aip.org/content/aip/journal/jap/119/9?ver=pdfcov>

Published by the [AIP Publishing](#)

Articles you may be interested in

[Co-implantation of Al⁺, P⁺, and S⁺ with Si⁺ implants into In_{0.53}Ga_{0.47}As](#)

[J. Vac. Sci. Technol. B](#) **33**, 051217 (2015); 10.1116/1.4931030

[Si doping effects on \(In,Ga\)N nanowires](#)

[J. Appl. Phys.](#) **116**, 244310 (2014); 10.1063/1.4905257

[Raman scattering in InAs nanowires synthesized by a solvothermal route](#)

[Appl. Phys. Lett.](#) **89**, 253117 (2006); 10.1063/1.2422897

[Raman study of As outgassing and damage induced by ion implantation in Zn -doped GaAs](#)

[J. Appl. Phys.](#) **96**, 4890 (2004); 10.1063/1.1803615

[Study of the electrical activation of Si + -implanted InGaAs by means of Raman scattering](#)

[J. Appl. Phys.](#) **93**, 2659 (2003); 10.1063/1.1542659

A promotional banner for AIP Applied Physics Reviews. The background is a dark blue gradient with a bright light source on the right, creating a lens flare effect. On the left, there is a small inset image of a book cover for 'AIP Applied Physics Reviews' featuring a diagram of a layered structure. The main text 'NEW Special Topic Sections' is in large, white, bold font. Below this, 'NOW ONLINE' is written in yellow, followed by 'Lithium Niobate Properties and Applications: Reviews of Emerging Trends' in white. The AIP Applied Physics Reviews logo is in the bottom right corner.

NEW Special Topic Sections

NOW ONLINE
Lithium Niobate Properties and Applications:
Reviews of Emerging Trends

AIP Applied Physics
Reviews

Activation of Si implants into InAs characterized by Raman scattering

A. G. Lind,^{1,a)} T. P. Martin, Jr.,¹ V. C. Sorg,² E. L. Kennon,¹ V. Q. Truong,¹ H. L. Aldridge,¹ C. Hatem,³ M. O. Thompson,⁴ and K. S. Jones¹

¹Department of Materials Science and Engineering, University of Florida, Gainesville, Florida 32611, USA

²School of Chemical and Biomolecular Engineering, Cornell University, Ithaca, New York 14853, USA

³Applied Materials, Gloucester, Massachusetts 01930, USA

⁴Department of Materials Science and Engineering, Cornell University, Ithaca, New York 14853, USA

(Received 23 September 2015; accepted 22 January 2016; published online 2 March 2016)

Studies of implant activation in InAs have not been reported presumably because of challenges associated with junction leakage. The activation of 20 keV, Si⁺ implants into lightly doped (001) p-type bulk InAs performed at 100 °C as a function of annealing time and temperature was measured via Raman scattering. Peak shift of the L₊ coupled phonon-plasmon mode after annealing at 700 °C shows that active n-type doping levels $\approx 5 \times 10^{19} \text{ cm}^{-3}$ are possible for ion implanted Si in InAs. These values are comparable to the highest reported active carrier concentrations of $8\text{--}12 \times 10^{19} \text{ cm}^{-3}$ for growth-doped n-InAs. Raman scattering is shown to be a viable, non-contact technique to measure active carrier concentration in instances where contact-based methods such as Hall effect produce erroneous measurements or junction leakage prevents the measurement of shallow n⁺ layers, which cannot be effectively isolated from the bulk. © 2016 AIP Publishing LLC. [<http://dx.doi.org/10.1063/1.4942880>]

INTRODUCTION

InAs has attracted a large amount of attention for future applications in nanowire FETs due to the high ballistic injection velocity^{1–3} and the more recent emphasis on low power devices such as tunnel FETs because of the high tunneling currents achievable in InAs heterojunction devices.^{4–7} Heavily n-doped source and drain regions are required to reduce contact resistances and subsequent degradation in on-state current in both of these device configurations. Previous studies of n-type doping in InAs generally report n-layer formation with Si is possible via growth^{8–10} and more recent reports have studied monolayer doping of InAs using S.¹¹ However, there are virtually no reports on the activation of Si implants into InAs. This has been attributed to erroneous Hall effect results associated with the poor junction isolation in implanted InAs.¹² More recent work has shown that it is possible to study the doping concentration in InGaAs using calibrated Raman spectroscopy and the goal of this work is to similarly apply calibrated Raman spectroscopy to investigate the activation of implanted Si in InAs.^{13–15}

EXPERIMENTAL

Commercially available, 500 μm thick, 3 in. Zn-doped InAs wafers with a background p-type concentration of $3 \times 10^{17} \text{ cm}^{-3}$ grown using the liquid encapsulated Czochralski process were implanted with 20 keV, Si⁺ over a range of doses from 1×10^{13} to $-1 \times 10^{15} \text{ cm}^{-2}$ at a 7° tilt and 25° rotation. Additionally, the implantation was performed at 100 °C to prevent amorphization. The ion implanter used in this work was an Applied Materials VIIsta Trident ribbon beam ion implanter operating with a beam current of 1.1 mA. Transmission electron

microscopy (TEM) was performed using a JEOL-2010F. Fig. 1(a) shows TEM of the postimplant microstructure observed in cross section for the highest dose, $1 \times 10^{15} \text{ cm}^{-2}$ Si⁺ implant indicating that the crystallinity of the InAs was preserved. This observation is consistent with other observations of the amorphization threshold of InAs being in excess of $1 \times 10^{15} \text{ cm}^{-2}$.^{16,17} The stopping range of ions in matter (SRIM)¹⁸ was used to estimate Si concentrations for the 20 keV implants shown in Fig. 1(b). All samples were encapsulated with 15 nm of Al₂O₃ at 250 °C via atomic layer deposition (ALD) with a Cambridge Nanotech-Fiji using an exposure mode recipe resulting in a deposition rate of 1.1 nm/h after ion implantation to prevent surface degradation upon subsequent annealing treatments. Rapid thermal annealing was performed with an AG Associates Heatpulse 4100 halogen lamp RTA with Ar ambient. A fixed ramp rate of 60 °C/s was used to reach the temperatures ranging from 400 to 700 °C and annealing times of 1–90 s were used to activate the implanted Si. Protective ALD Al₂O₃ layers were stripped with HF prior to Raman measurements. Van der Pauw Hall effect measurements are frequently used to measure the active dose of implanted semiconducting materials after thermal treatment but van der Pauw Hall effect measurements of 20 keV, $1 \times 10^{14} \text{ cm}^{-2}$ Si⁺ implants into bulk InAs treated with a 700 °C, 5 s RTA resulted in background p-type sheet carrier concentrations equivalent to the as-grown InAs material. This result is consistent with previous work,¹⁹ which showed no discernable activation beyond the background p-type doping of the sample presumably due to junction leakage.²⁰ Other reports of surface inversion layers of InAs have resulted in measurement complications for InAs heterostructures as well.⁹ The reported complications of measuring electrical activation of implanted dopants into InAs via Hall effect may explain the lack of previous reports of dopant activation despite n-type implants being performed

^{a)}Author to whom correspondence should be addressed. Electronic mail: aglind@ufl.edu

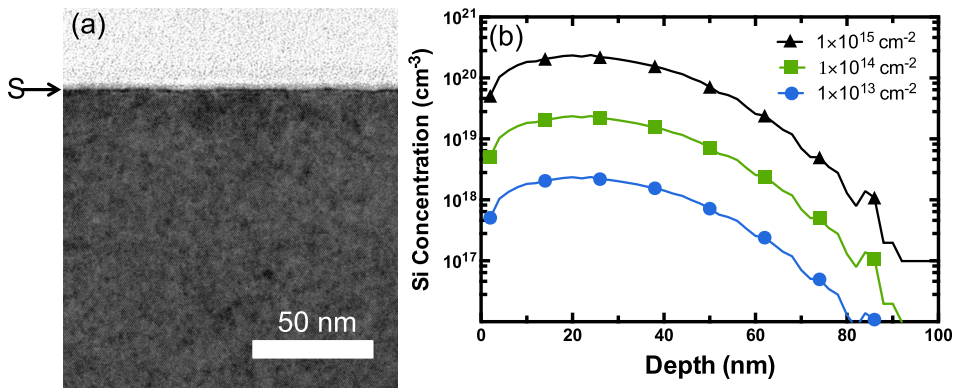


FIG. 1. (a) Post-implant cross-sectional TEM (XTEM) of 20 keV, $1 \times 10^{15} \text{ cm}^{-2}$ Si^+ implant performed at 100°C . The surface of the implanted InAs is indicated by “S.” (b) Calculated Si concentration profiles for 20 keV Si^+ implant at varying implant doses.

in earlier works. For this reason, non-contact optical methods of carrier concentration were used to measure Si activation for a range of annealing times and temperatures.

Previous authors have used Raman scattering to measure free carrier concentrations making use of the fact that LO phonons will readily couple with the plasma oscillations of free carriers in InAs and other polar, III-V materials.^{13,14,21–27} The L_+ phonon-plasmon coupled mode is especially sensitive to changes in the carrier concentration at high n-type carrier concentrations in InAs where Raman shifts towards higher wavenumbers correspond to increasing free electron concentrations. Diffusion of Si in InAs beyond the initial implanted profile may increase the active sheet number measured by Hall effect precluding accurate carrier concentration estimates without corresponding Si diffusion data. However, the active carrier concentration estimated from Raman shift of L_+ and L_- modes is primarily sensitive to the peak carrier concentration and will be minimally influenced by active carriers in lower concentration regions formed by extended diffusion. Raman spectroscopy for this study was performed with a 532 nm laser on a Horiba Jobin-Yvon LabRAM Aramis using a grating pitch of 1800 g/mm with a charge coupled detector. All subsequently reported Raman shifts are relative to the Rayleigh line of the 532 nm laser. The probing depth at this wavelength ($1/2\alpha$) was calculated to be 21.4 nm based on the data for InAs collected by Aspnes *et al.*²⁸ The projected range of the implant is calculated to be 26 nm based on SRIM. Previous work done to correlate the peak shift of a L_+ phonon-plasmon mode to active carrier concentrations measured by Hall effect on MBE grown n-InAs on GaAs by Li *et al.*²⁷ was used to estimate the maximum active carrier concentration in this work. The work by Li *et al.* fits a smooth calibration curve to three measurements of active carrier concentration from $9 \times 10^{18} \text{ cm}^{-3}$ to $4 \times 10^{19} \text{ cm}^{-3}$. Quadratic interpolation between these previously reported values will inevitably result in some uncertainty in active concentration values estimated from the measured Raman shift. It is especially difficult to accurately estimate the carrier concentration for Raman shifts that are extrapolations of their data.

RESULTS

Fig. 2(a) shows the Raman scattering intensity as a function of wavenumber relative to the Rayleigh line for the L_+ coupled mode for 30 s anneals ranging from 400 to 700°C

for the 20 keV $1 \times 10^{15} \text{ cm}^{-2}$ Si^+ implants. The L_+ phonon-coupling mode is shown to shift towards higher wavenumbers with increasing annealing temperature. Fig. 2(b) more clearly shows the peak shift of L_- and LO modes with increasing annealing temperature. Annealing temperatures below 500°C result in no significant L_+ Raman shift over that of the as implanted or as grown wafer, indicating that anneals at 500°C are required to result in significant activation of the implanted dopants. A peak shift of the L_- mode indicates that anneals as low as 400°C still result in activation of implanted dopants to values less than $1 \times 10^{19} \text{ cm}^{-3}$. The observed intensity ratio of the L_-/L_+ modes for the obtained spectra of the 700°C and 400°C anneals was 8 and 30, respectively. The measured peak shift of the L_+ coupled mode for the 30 s anneal at 700°C is shown to be approximately 1660 cm^{-1} . The estimated active carrier concentrations in these samples based on the results by Yi *et al.* are shown in Fig. 3. The highest annealing temperature of 700°C resulted in an estimated peak concentration of $4.9 \times 10^{19} \text{ cm}^{-3}$. Figs. 4(a) and 4(b) show the effect of implanted dose on electrical activation for a 30 s, 700°C RTA. The L_+ peak shift is shown to move toward higher wavenumbers with increasing implant dose, indicating that higher implant doses resulted in higher active carrier concentrations. The lowest dose, $1 \times 10^{13} \text{ cm}^{-2}$ implant, shows no evidence of n-type activation. This result is not surprising given that the peak Si concentration in this case is roughly $2.3 \times 10^{18} \text{ cm}^{-3}$. The background p-type concentration of the InAs is $3 \times 10^{17} \text{ cm}^{-3}$. This suggests that for the lowest dose studied, a 30 s RTA at 700°C was not able to activate enough of the implanted dopants to overcome the background p-type doping. The estimated carrier concentration for the variable dose implants annealed at 700°C for 30 s is shown in Fig. 5. An isothermal annealing experiment with times ranging from 1 to 90 s was also performed for varying anneal temperatures for the $1 \times 10^{15} \text{ cm}^{-2}$ dose implant. The L_+ peak shifts as a function of annealing time are shown in Fig. 6. The longest annealing time of 90 s resulted in a peak shift of 1720 cm^{-1} , which corresponds to an active carrier concentration $>5 \times 10^{19} \text{ cm}^{-3}$ based on the results of Li *et al.* Experimental measurements of carrier concentrations for Raman shifts above 1600 cm^{-1} in InAs have not been reported and it is not well understood how conduction band non-parabolicity may affect the observed Raman shift at high carrier concentrations. As such, it is difficult to properly

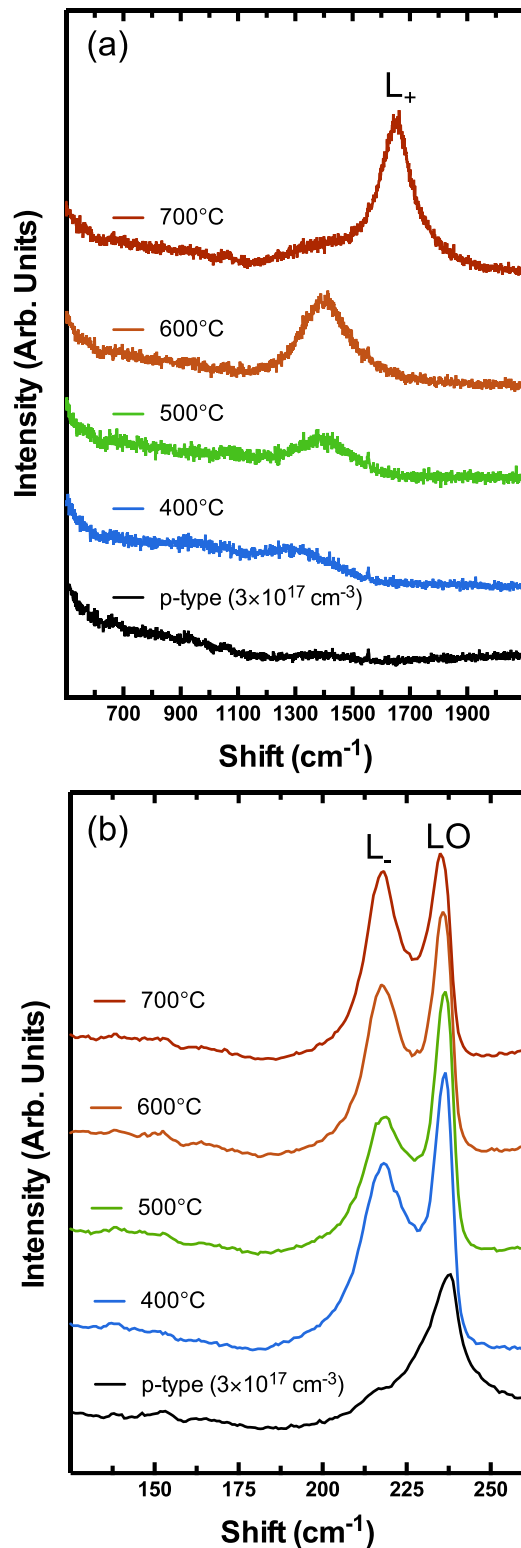


FIG. 2. Intensity as a function of Raman shift for InAs with a 20 keV, $1 \times 10^{15} \text{ cm}^{-2}$ Si^+ implant performed at 100°C after annealing for various temperatures from 400 to 700°C . From (a) 500 to 2100 cm^{-1} emphasizing the L_+ mode and (b) 125 to 260 cm^{-1} emphasizing the L_- and LO modes.

estimate carrier concentrations above $5 \times 10^{19} \text{ cm}^{-3}$. The estimated active carrier concentration for the isochronal annealing from 1 to 90 s is shown in Fig. 7 and increasing annealing times at 700°C are shown to steadily increase the free carrier concentration.

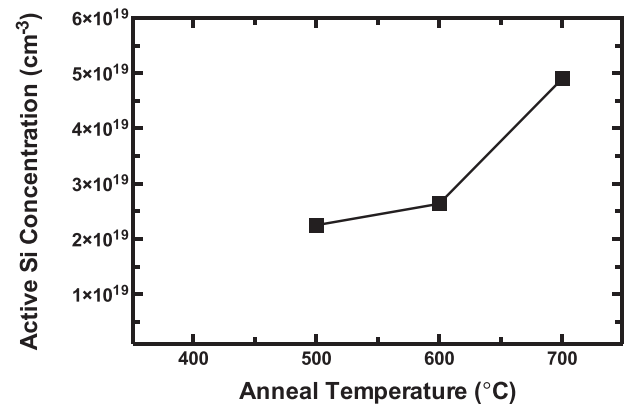


FIG. 3. Active Si concentration as a function of annealing temperature for a 30 s RTA of a 20 keV, $1 \times 10^{15} \text{ cm}^{-2}$ Si^+ implant performed at 100°C .

DISCUSSION

Previous studies of electrically active implants into InAs have not shown significant activation of the implanted materials despite very high doses of electrically active implants being used.^{19,29} Other studies of ion implanted n-type impurities focus on damage production in these materials.³⁰ The attempt to measure activation via Hall effect resulted in no observation of Si activation, consistent with attempts by previous experimenters,¹⁹ and this difficulty may explain the lack of data on activation of implants into bulk InAs and other semiconductors despite a number of studies performing n-type dopant implants into InAs. Activation of implants with annealing temperatures above 400°C are consistent with reports that these annealing temperatures are required to recover damage due to ion implantation and cause subsequent movement of dopants onto lattice sites.³¹ Previous studies have indicated that anneals above 600°C results in conversion from n-type activation of Ge and Si implants to p-type¹⁹ based on photoluminescence results, but these earlier results are suspicious, given that no type conversion was observed based on the Raman shift in this work. The lack of type conversion even at high annealing temperatures in this work and may indicate that at high annealing temperatures surface degradation or some other effect led to the spurious peak shift in the photoluminescence spectra.

The maximum reported activation for growth-doped InAs substrates is $6\text{--}12 \times 10^{19} \text{ cm}^{-3}$.^{10,32} Implanted Si is shown to activate up to $5 \times 10^{19} \text{ cm}^{-3}$ in this work. The observation of decreased activation for implanted material relative to growth-doped material by other experimenters is consistent with other reports of n-type dopants in III-V arsenides. In the case of GaAs and $\text{In}_{0.53}\text{Ga}_{0.47}\text{As}$, previous reports indicate that the maximum active carrier concentration achievable in these materials is much higher for MBE and metal organic chemical vapor deposition (MOCVD) growth-doped substrates than implant doped substrates.^{33,34}

Heavy n-type doping of III-V arsenides generally results in significant concentrations of compensated carriers and prior MBE experiments report that Si doping $> 1 \times 10^{20}$ was necessary to create layers with active carrier concentrations of

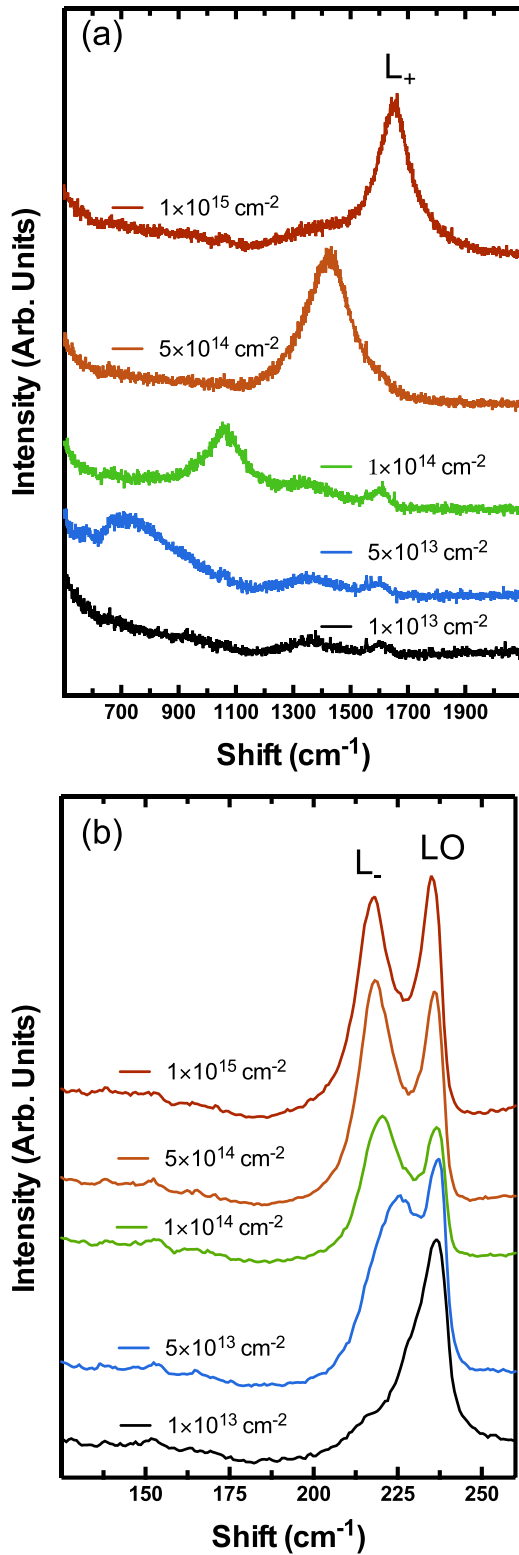


FIG. 4. Intensity as a function of Raman shift for InAs with a 20 keV, Si⁺ implant performed at 100 °C after annealing at 700 °C for 30 s for doses ranging from $1 \times 10^{13} \text{ cm}^{-2}$ to $1 \times 10^{15} \text{ cm}^{-2}$. From (a) 500 to 2100 cm^{-1} highlighting the L₊ mode and (b) the L₋ and LO modes from 125 to 260 cm^{-1} .

$6 \times 10^{19} \text{ cm}^{-3}$ (Refs. 10 and 32) and $3.5 \times 10^{20} \text{ cm}^{-3}$ for an active carrier concentration of $1.2 \times 10^{20} \text{ cm}^{-3}$, indicating a high concentration of electrically inactive Si. The peak of the as-implanted Si concentration for the various implant doses in

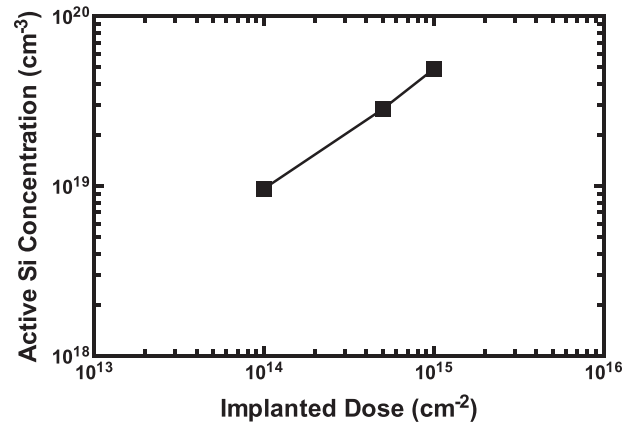


FIG. 5. Active Si concentration as a function of implanted dose for a 700 °C, 30 s RTA for a 20 keV, $1 \times 10^{15} \text{ cm}^{-2}$ Si⁺ implant performed at 100 °C.

this work were estimated using SRIM shown in Fig. 1(b). The highest implant dose of $1 \times 10^{15} \text{ cm}^{-2}$ results in a peak Si concentration of $2.3 \times 10^{20} \text{ cm}^{-3}$, which is much higher than the observed Si activation level of $\approx 5 \times 10^{19}$. If minimal Si redistribution upon annealing is assumed, the large difference in active concentration and the implanted peak concentration suggests that some Si is inactive after implantation and annealing. The activation levels observed in this report is still significantly higher than the activation levels achieved by previous S monolayer doping, suggesting Si implantation is an effective means to create heavily doped, n-type InAs.

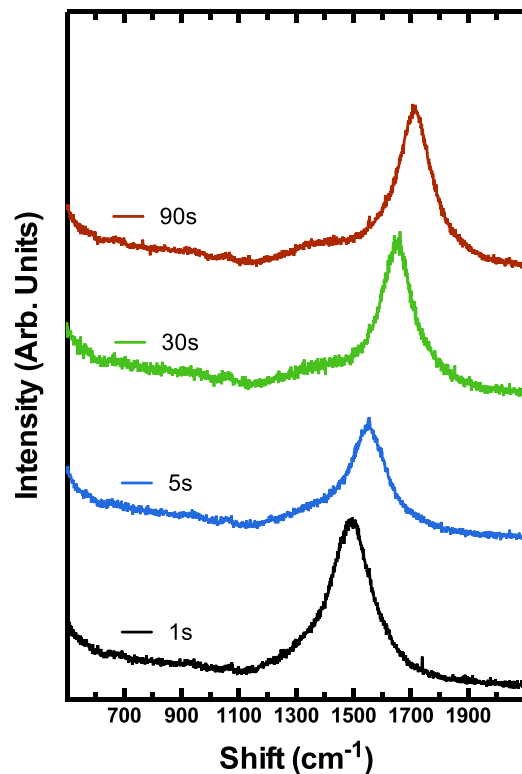


FIG. 6. Intensity as a function of Raman shift for InAs with a 20 keV, $1 \times 10^{15} \text{ cm}^{-2}$ Si⁺ implant performed at 100 °C after annealing at 700 °C for times ranging from 1 to 90 s.

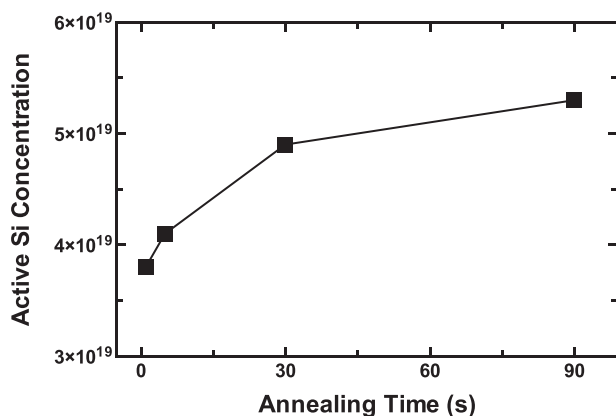


FIG. 7. Active Si concentration as a function of annealing time for InAs with a 20 keV, $1 \times 10^{15} \text{ cm}^{-2}$ Si^+ implant performed at 100 °C after annealing at 700 °C for times ranging from 1 to 90 s.

CONCLUSIONS

In conclusion, Si implants into bulk InAs were shown to activate as high as $5 \times 10^{19} \text{ cm}^{-3}$, and this activation level is to our knowledge the first report of significant n-type activation from ion implantation in InAs. Efforts to characterize electrical activation of shallow Si implants into bulk InAs via Hall effect were unsuccessful, but scattering of the L_+ phonon-plasmon mode in Raman spectroscopy clearly shows activation and the creation of heavily n-type layers after implantation and subsequent thermal annealing of 400 °C or more for a wide range of implant doses.

ACKNOWLEDGMENTS

The authors would like to acknowledge the Major Analytical Instrumentation Center at UF for the use of their transmission electron microscopy and FIB facilities as well as the Nanoscale Research Facility for the use of the micro Raman system.

¹J. A. del Alamo, *Nature* **479**, 317 (2011).

²E. Lind, A. I. Persson, L. Samuelson, and L.-E. Wernersson, *Nano Lett.* **6**, 1842 (2006).

³S. Chuang, Q. Gao, R. Kapadia, A. C. Ford, J. Guo, and A. Javey, *Nano Lett.* **13**, 555 (2013).

⁴B. M. Borg, M. Ek, B. Ganjipour, A. W. Dey, K. A. Dick, L.-E. Wernersson, and C. Thelander, *Appl. Phys. Lett.* **101**, 043508 (2012).

⁵A. C. Ford, C. W. Yeung, S. Chuang, H. S. Kim, E. Plis, S. Krishna, C. Hu, and A. Javey, *Appl. Phys. Lett.* **98**, 113105 (2011).

⁶K. Ganapathi, Y. Yoon, and S. Salahuddin, *Appl. Phys. Lett.* **97**, 033504 (2010).

⁷A. M. Ionescu and H. Riel, *Nature* **479**, 329 (2011).

⁸S. Y. Kim, J. D. Song, and T. W. Kim, *J. Korean Phys. Soc.* **58**, 1347 (2011).

⁹L. Botha, P. Shamba, and J. R. Botha, *Phys. Status Solidi C* **5**, 620 (2008).

¹⁰P. D. Wang, S. N. Holmes, T. Le, R. A. Stradling, I. T. Ferguson, and A. G. de Oliveira, *Semicond. Sci. Technol.* **7**, 767 (1992).

¹¹J. C. Ho, A. C. Ford, Y.-L. Chueh, P. W. Leu, O. Ergen, K. Takei, G. Smith, P. Majhi, J. Bennett, and A. Javey, *Appl. Phys. Lett.* **95**, 072108 (2009).

¹²M. I. Guseva, N. V. Zotova, A. V. Koval, and D. N. Nasledov, *Sov. Phys. Semicond.* **8**, 59 (1974).

¹³K. R. Kort, P. Y. Hung, P. D. Lysaght, W.-Y. Loh, G. Bersuker, and S. Banerjee, *Phys. Chem. Chem. Phys.* **16**, 6539 (2014).

¹⁴S. Hernández, R. Cuscó, N. Blanco, G. González-Dríguez, and L. Artús, *J. Appl. Phys.* **93**, 2659 (2003).

¹⁵V. Sorg, S. N. Zhang, M. Hill, P. Clancy, and M. O. Thompson, *ECS Trans.* **66**, 117 (2015).

¹⁶W. Wesch and M. C. Ridgway, *Mater. Sci. Semicond. Process.* **7**, 35 (2004).

¹⁷Z. Hussain, E. Wendler, W. Wesch, G. Foran, C. Schnohr, D. Llewellyn, and M. Ridgway, *Phys. Rev. B* **79**, 085202 (2009).

¹⁸J. F. Ziegler, M. D. Ziegler, and J. P. Biersack, *Nucl. Instrum. Methods Phys. Res., Sect. B* **268**, 1818 (2010).

¹⁹M. I. Guseva, N. V. Zotova, A. V. Koval, and D. N. Nasledov, *Behavior of Group IV Elements Introduced Into Indium Arsenide by Ion Implantation* (Soviet Semiconductor Physics, 1974).

²⁰S. H. Jain, P. B. Griffin, and J. D. Plummer, *J. Appl. Phys.* **93**, 1060 (2003).

²¹K. R. Kort, P. Y. Hung, W. Y. Loh, and G. Bersuker, *Appl. Spectrosc.* **69**(2), 239 (2015).

²²L. P. Avakyants and T. P. Kolmakova, *Inorg. Mater.* **47**, 335 (2011).

²³R. Cuscó, L. Artús, S. Hernández, J. Ibáñez, and M. Hopkinson, *Phys. Rev. B* **65**, 035210 (2001).

²⁴J. E. Maslar, J. F. Dorsten, P. W. Bohn, and S. Agarwala, *Phys. Rev. B* **50**(23), 17143 (1994).

²⁵T. Yuasa, S. Naritsuka, M. Mannoh, and K. Shinozaki, *Phys. Rev. B* **33**, 1222 (1986).

²⁶H. Kamioka, S. Saito, and T. Suemoto, *J. Lumin.* **87–89**, 923 (2000).

²⁷Y. B. Li, I. T. Ferguson, R. A. Stradling, and R. Zallen, *Semicond. Sci. Technol.* **7**, 1149 (1992).

²⁸D. E. Aspnes and A. A. Studna, *Phys. Rev. B* **27**, 985 (1983).

²⁹N. N. Gerasimenko, A. M. Myasnikov, A. A. Nesterov, V. I. Obodnikov, L. N. Safronov, and G. S. Khriashev, *Nucl. Instrum. Methods Phys. Res., Sect. B* **39**, 480 (1989).

³⁰S. J. Pearton, A. R. Von Neida, J. M. Brown, K. T. Short, L. J. Oster, and U. K. Chakrabarti, *J. Appl. Phys.* **64**, 629 (1988).

³¹S. J. Pearton, *Int. J. Mod. Phys. B* **7**, 4687 (1993).

³²A. Baraskar, V. Jain, and M. A. Wistey, in *Proceedings of the International Conference on Indium Phosphide and Related Compounds* (2010), p. 1.

³³A. G. Lind, H. L. Aldridge, Jr., C. C. Bomberger, C. Hatem, J. M. O. Zide, and K. S. Jones, *J. Vac. Sci. Technol., B* **33**, 021206 (2015).

³⁴T. Orzali, A. Vert, R. Lee, A. Norvilas, and G. Huang, *J. Cryst. Growth* **426**, 243 (2015).